

Adaptive Genetic Algorithm for Crystal Structure Prediction

S Q Wu^{1,2}, M Ji², C Z Wang², M C Nguyen², X Zhao², K Umemoto^{2,3}, R M Wentzcovitch⁴ and K M Ho²,

¹ Department of Physics, Xiamen University, Xiamen 361005, China

² Ames Laboratory - US DOE and Department of Physics and Astronomy, Iowa State University, Ames, Iowa 50011, USA

³ Department of Earth Sciences, University of Minnesota, Minneapolis, MN 55455, USA

⁴ Minnesota Supercomputing Institute and Department of Chemical Engineering and Materials Science, University of Minnesota, Minneapolis, MN 55455, USA

E-mail: wangcz@ameslab.gov (C Z Wang), kmh@ameslab.gov (K M Ho)

Abstract. We present a genetic algorithm (GA) for structural search that combines the speed of structure exploration by classical potentials with the accuracy of density functional theory (DFT) calculations in an adaptive and iterative way. This strategy increases the efficiency of the DFT-based GA by several orders of magnitude. This gain allows considerable increase in size and complexity of systems that can be studied by first principles. The method's performance is illustrated by successful structure identifications of complex binary and ternary inter-metallic compounds with 36 and 54 atoms per cell, respectively. The discovery of a multi-TPa Mg-silicate phase with unit cell containing up to 56 atoms is also reported. Such phase is likely to be an essential component of terrestrial exoplanetary mantles.

(Some figures may appear in colour only in the online journal)

PACS numbers: 61.50.Ah, 61.50.Ks, 91.60.Gf

Submitted to Journal of Physics: Condensed Matter

Crystal structure prediction starting from the chemical composition alone has been one of the long-standing challenges in theoretical solid state physics, chemistry, and materials science [1,2]. Progress in this area has become a pressing issue in the age of computational materials discovery and design. In the past two decades several computational methods have been proposed to tackle this problem. These

methods include simulated annealing [3-5], genetic algorithm (GA) [6-13], basin (or minima) hopping [14,15], particle swarm optimization [16,17], and *ab initio* random structure search [18]. While there has been steady progress in predicting crystal structures of elementary crystals, oxides, and binary alloys [8-13,16-18], exploration of complex binary, ternary, and quaternary systems has required more advanced algorithms for configuration space exploration and faster but reliable methods for energy evaluation. While first-principles density functional theory (DFT) calculations offer accurate total energies, its computational cost imposes the bottleneck to the structure identification of complex materials with unit cells containing $\sim 10^2$ atoms and/or with variable stoichiometries. By contrast, calculations based on classical potentials are fast and applicable to very large systems but are limited in accuracy. For various systems, reliable classical potentials are not even available. We present in this letter an *adaptive-GA* that combines the speed of classical potential searches and the accuracy of first-principles DFT calculations. It allows us to investigate crystal structures previously intractable by such methods with current computer capabilities.

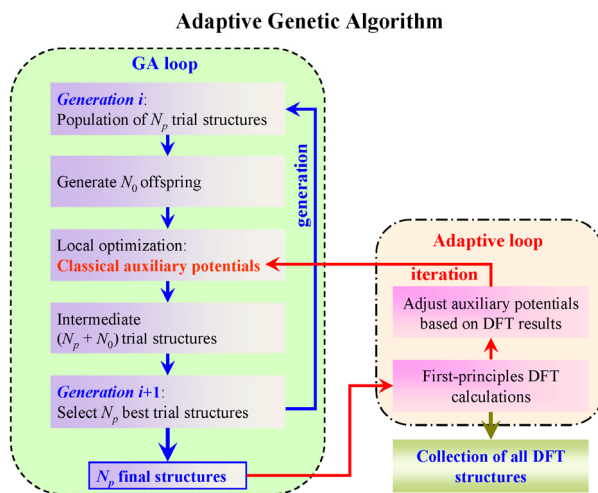


Figure 1. Flowchart of the adaptive genetic algorithm. The regular GA-loop is embedded in an adaptive loop. Optimization of offspring structures in the GA loop are performed using auxiliary classical potentials whose parameters are adjusted to reproduce DFT results obtained only in the adaptive loop.

The flowchart of the *adaptive*-GA scheme is illustrated in figure 1. The left-hand side of the flowchart is the traditional GA loop. The GA is an optimization strategy inspired by the Darwinian evolutionary process and has been widely adopted for atomistic structure optimization in the last 18 years [6-13]. During the GA optimization process, inheritance, mutation, selection, and crossover operations [6-13] are included to produce new structures and select most fit survivors from generation to generation. The most time-consuming step in the traditional GA-loop is the local optimization of new off-springs by DFT calculations. For complex structures, GA search usually iterates over 200 generations to converge. In the *adaptive*-GA scheme this most time-consuming step is performed using auxiliary classical potentials. In the *adaptive*-loop (see figure 1), single point DFT calculations are performed on a small set of candidate structures obtained in the GA-loop using the auxiliary classical potentials. Energies, forces, and stresses of these structures from first-principles DFT calculations are used to update the parameters of the auxiliary classical potentials by force-matching method with stochastic simulated annealing algorithm as implemented in the *potfit* code [19,20]. Another cycle of GA search is performed using the newly adjusted potentials, followed by the re-adjustment of the potential parameters, and the process is then repeated – an adaptive-GA (AGA) iteration. All first-principles DFT calculations were performed using the Quantum-ESPRESSO [21] or VASP [22,23], which has been interfaced with the adaptive-GA scheme in a fully parallel manner.

The numbers of parent, N_p , and off-spring structures, N_o , depend on the complexity of the system investigated. For those investigated here, $60 < N_o < 200$, and the total number of structures optimized in each GA-cycle varied between $\sim 12,000$ to $\sim 40,000$. The use of classical auxiliary potentials for such structure relaxations reduced the computational load by approximately five to six orders of magnitude. It usually takes 30-50 adaptive-GA-iterations to obtain the final structures and the net computational time of the entire adaptive-GA search can be reduced by more than three orders of magnitude. Since the classical potentials are adjusted according to DFT results, the adaptive-GA can explore configuration space more effectively. Structures collected over all adaptive-GA iterations and a set of low-energy metastable structures can be finally screened to locate the ground-state crystal structure. Therefore, the adaptive-GA

can essentially search for structures almost with the efficiency of classical potentials but with DFT accuracy.

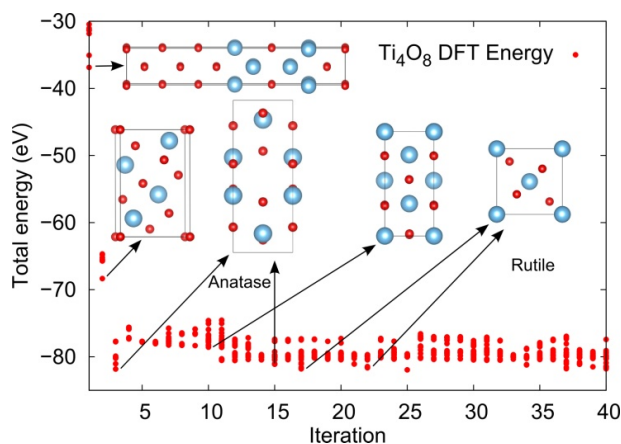


Figure 2. Structural and energetic evolution of TiO_2 versus iteration number of the AGA-loop. EAM-type potentials were used in inner GA-loop. Plots show only DFT energies obtained at the end of each AGA-iteration. The two low-energy crystal structures of TiO_2 , *i.e.*, the rutile and the anatase structures could be obtained within 25 AGA-iterations.

We note that the commonly adopted approach of combining classical potentials with DFT calculations for structure optimization involves the use of a *single* set of classical potentials to screen *all* candidate structures followed by a refinement using DFT calculations. This requires accurate and transferable classical potentials able to capture the very-lowest (or few low) energy structures in a complex energy landscape. In contrast, from the energies of the final structures at each iteration as plotted in Fig 2 (and Fig 3 in the following), we can see that the adaptive-GA uses different adjusted potentials to sample structures located in different basins of the energy landscape. Each auxiliary classical potential may not just sample the structures in the same basin, it can sample the structures in a subset of the basins in the energy landscape and some of the basins may overlap with those from other potentials. Therefore adaptive GA is not designed to fit transferable potentials for general atomistic simulations. It is very difficult or even impossible to fit a classical potential able to accurately describe a system under various

bonding environments, especially for binary and ternary systems. However, it is possible to adjust auxiliary potentials to describe structures located within different subset of basins in the energy landscape with DFT accuracy. Adapted auxiliary potentials adjusted throughout the adaptive-GA-iterations help the system to hop between basins and ensure efficient and accurate sampling of configuration space. An illustration of this point is the search for the crystal structure of TiO_2 with Embedded-atom method (EAM) type potentials. We do not expect EAM potentials to describe well the energies of various TiO_2 polymorphs. However, as seen in figure 2, the adaptive-GA search for structures with 4 formula units (12 atoms per unit cell) was able to find the two low-energy structures of TiO_2 , *i.e.*, the rutile [24] and the anatase [25] structures – both with 6 atoms per primitive cell only – within 25 adaptive-GA-iterations. The theoretical structural parameters of the rutile and the anatase TiO_2 together with the experimental values are given in table 1.

Table 1. Structural parameters of Rutile & Anatase TiO_2

TiO_2		Theo.	Expt.[24]
Space group			Rutile
(a, c) (Å)			$P4_2/mnm$
Ti	2a	(4.6501, 2.9697)	(4.5929, 2.9591)
O	4f	(0.0000, 0.0000, 0.0000)	(0, 0, 0)
		(0.3049, 0.3049, 0.0000)	(0.3056, 0.3056, 0)
Space group			Anatase
(a, c) (Å)			$I4_1/amd$
Ti	4a	(3.8074, 9.7050)	(3.785, 9.514)
O	8e	(0.0000, 0.0000, 0.0000)	(0, 0, 0)
		(0.0000, 0.0000, 0.2067)	(0, 0, 0.2064)

To validate the adaptive-GA for complex crystal structure prediction we searched for structures of the Hf_2Co_7 binary alloy with 36 atoms per unit cell and of the ZrCo_3B_2 ternary alloy with 54 atoms per unit cell. Ground-state structures of these alloys have been well characterized experimentally [26, 27]. The adaptive-GA searches were performed using only chemical compositions as input information. Initial parent structures were generated by placing atoms randomly in the unit cell. EAM-type potentials were

used in the GA-loop. As shown in figure 3, initially the unit cell shapes, atomic positions, and energies of Hf_2Co_7 and ZrCo_3B_2 structures are far from the ground-state. Adaptive-GA searches then quickly locate the correct ground-state structures for these alloys within 8 and 15 iterations, respectively. The predicted and experimental structural parameters for these two structures are presented in table 2 & 3. Note that for the ZrCo_3B_2 , once the experimental structure ($R-3$) is relaxed by DFT method, a higher symmetry ($R-3m$) can be obtained. The $R-3m$ structure is the ground state structure predicted by our adaptive-GA searches. These results demonstrate the power of the adaptive-GA as a computational tool for predicting complex crystal structures.

Table 2. Structural parameters of Hf_2Co_7

Hf_2Co_7		Theo.	Expt.[26]
Space group			$C2/m$
(a, b, c) (Å)		(4.6513, 8.2302, 12.0853)	(4.444, 8.191, 12.14)
β (°)		84.4110	90
Hf(1)	4i	(0.2187, 0.0000, 0.8830)	(0.27, 0, 0.884)
Hf(2)	4i	(0.2857, 0.0000, 0.6172)	(0.212, 0, 0.613)
Co(1)	8j	(-0.0025, 0.2499, 0.2499)	(0.053, 0.246, 0.251)
Co(2)	8j	(0.2953, 0.1663, 0.0769)	(0.208, 0.162, 0.076)
Co(3)	8i	(0.2006, 0.1664, 0.4232)	(0.297, 0.168, 0.421)
Co(4)	4i	(0.2474, 0.0000, 0.2502)	(0.256, 0, 0.246)

Table 3. Structural parameters of ZrCo_3B_2

ZrCo_3B_2		Theo.	Expt.[27]
Space group		$R-3m$	$R-3$
(a, c) (Å)		(8.4171, 9.0415)	(8.418, 9.132)
Zr(1)	3a	(0.0000, 0.0000, 0.0000)	(0, 0, 0)
Zr(2)	6c	(0.0000, 0.0000, 0.3304)	(0, 0, 0.328)
Co(1)	9d	(0.5000, 0.0000, 0.5000)	(0.5, 0, 0.5)
Co(2)	18h/18f	(0.1674, 0.8326, 0.1387)	(0.169, 0.834, 0.136)
B	18f	(0.3756, 0.0000, 0.0000)	(0.072, 0.727, 0.33)

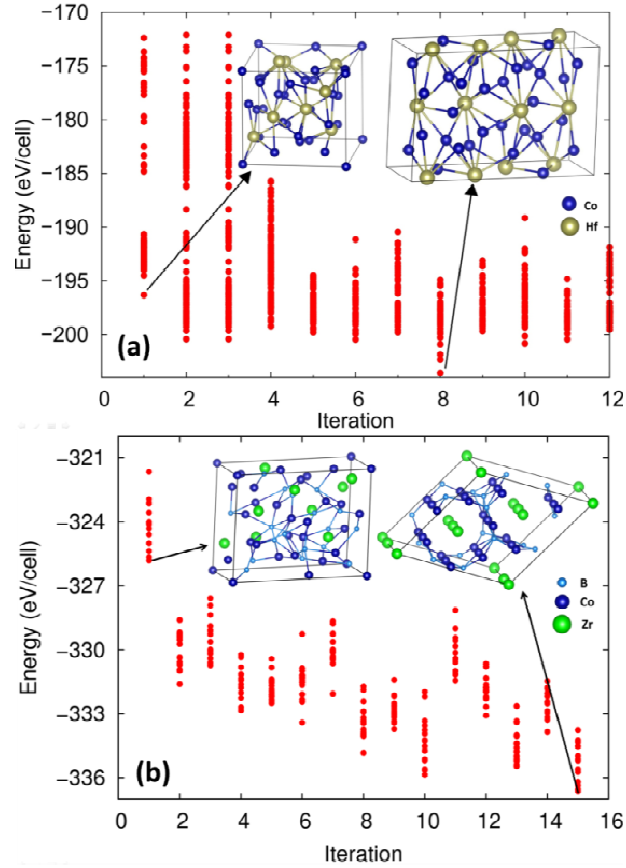
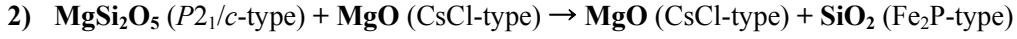
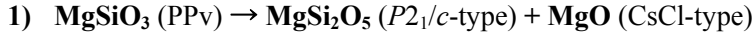


Figure 3. Structural and energetic evolution versus iteration number of the AGA-loop for (a) Hf_2Co_7 and (b) ZrCo_3B_2 alloys. EAM-type potentials were used in inner GA-loop. Plots show only DFT energies obtained at the end of each AGA-iteration.

Materials discovery is a very active area of research in mineral physics. This is motivated by the discovery of a myriad of candidates of "super-Earths" whose densities are comparable to Earth's and masses are 1~10 times Earth's mass by Kepler [28] and CoRoT [29] missions. MgSiO_3 perovskite (Pv) is the most abundant mineral phase in Earth's lower mantle. In 2004, a post-perovskite phase (PPv) was stabilized by subjecting MgSiO_3 -Pv to ~ 125 GPa and $\sim 2,500$ K [30]. The Pv \rightarrow PPv transition [30-32] in MgSiO_3 seems to be associated with a major seismic discontinuity in the mantle at ~ 250 km above the core mantle boundary – the D'' discontinuity. Although the PPv phase is the final form of MgSiO_3 in the Earth, further phase transitions are expected to occur in super-Earths. The dissociation of MgSiO_3 -PPv

into elementary oxides, SiO₂ and MgO, was then predicted to take place at ~1.1 TPa [33]. A more gradual dissociation process, a two-step ex-solution of MgO from MgSiO₃, has recently been identified [34]:



This has raised new questions about the complexity of the dissociation process. Clarification of this process and of the nature of intermediate aggregates is essential for understanding the internal structure of terrestrial-type exoplanets. It is also relevant for advancing knowledge of the dense cores of the giant planets, which should contain these most abundant Earth forming elements in condensed form.

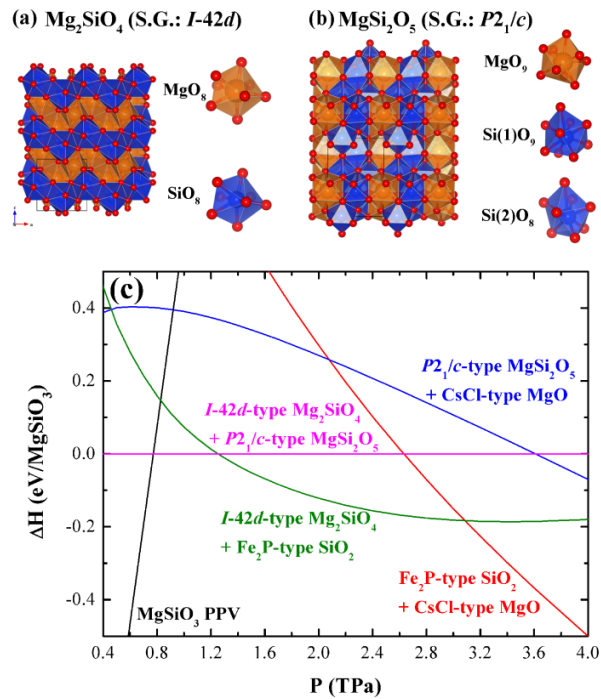


Figure 4. Crystal structures of (a) $I-42d$ Mg_2SiO_4 and (b) $P2_1/c$ MgSi_2O_5 ; (c) Relative enthalpies of MgSiO_3 PPv, aggregations of $I-42d$ -type Mg_2SiO_4 and Fe₂P-type SiO₂, of $P2_1/c$ -type MgSi_2O_5 and CsCl-type MgO, and of CsCl-type MgO and Fe₂P-type SiO₂ with respect to an aggregation of $I-42d$ -type Mg_2SiO_4 and $P2_1/c$ -type MgSi_2O_5 .

Here we have searched for phases in an enlarged composition space and considered also the gradual ex-solution of SiO₂ from MgSiO₃:



The adaptive-GA was used to investigate possible dissociation pathways involving stepwise ex-solutions of SiO₂ and/or of MgO up to ~ 4TPa. This required predictions of crystal structures for various phases with these compositions and unit cells containing up to 56 atoms (8 formula unit of Mg₂SiO₄).

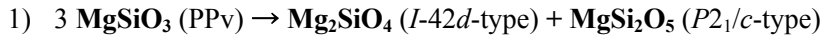
Table 4. Structural parameters of *I-42d* Mg₂SiO₄ and *P2₁/c* MgSi₂O₅ at 1 TPa

Mg ₂ SiO ₄		
Space group		<i>I-42d</i>
(<i>a, c</i>) (Å)		(4.5745, 4.7006)
Mg	8d	(0.1118, 0.2500, 0.1250)
Si	4b	(0.0000, 0.0000, 0.5000)
O	16e	(0.4310, 0.3139, 0.2968)
MgSi ₂ O ₅		
Space group		<i>P2₁/c</i>
(<i>a, b, c</i>) (Å)		(4.4358, 4.0308, 6.1897)
<i>β</i> (°)		89.5808
Mg	4e	(0.0056, 0.5641, 0.1688)
Si(1)	4e	(0.5032, 0.4519, 0.8240)
Si(2)	4e	(0.7569, 0.9309, 0.9917)
O(1)	4e	(0.7385, 0.6749, 0.7195)
O(2)	4e	(0.2678, 0.8453, 0.1942)
O(3)	4e	(0.7263, 0.5331, 0.0000)
O(4)	4e	(0.9575, 0.1890, 0.0776)
O(5)	4e	(0.4606, 0.8275, 0.9139)

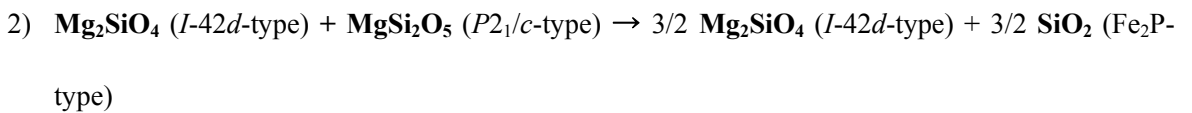
Results confirm the stability of all structures previously identified in the dissociation pathway of MgSiO₃ [13, 33, 34]. The intermediate SiO₂- and MgO-rich compounds we now include are MgSi₂O₅, and Mg₂SiO₄. A previous structural search on Mg₂SiO₅ was done following soft phonon modes [34]. Here the search for structures is more thorough using the adaptive-GA. MgO undergoes a pressure induced transition from NaCl-type to a CsCl-type phase at ~0.53 TPa, consistent with other first-principles calculations [35-38]. SiO₂ undergoes a phase transition from pyrite- to a Fe₂P-type phase at ~0.69 TPa [13, 39]. The previously predicted structure of MgSi₂O₅ is *P2₁/c*-type [34] and has 32 atoms per cell. The AGA

search carried out using up to 48 atoms per cell confirms this $P2_1/c$ -type phase to be the lowest-enthalpy phase at the high pressures considered here. Here we predicted a new high-pressure phase of Mg_2SiO_4 . This structure is body-centered-tetragonal with space group $I-42d$. Hereafter, we refer to this phase as $I-42d$ -type Mg_2SiO_4 . As far as we know, this structure has not been identified in any substance. However, its cation configuration is identical to that of Zn_2SiO_4 -II whose space group is $I-42d$ also [40]. The difference between $I-42d$ -type Mg_2SiO_4 and Zn_2SiO_4 -II structures is in the oxygen arrangement. $I-42d$ -type Mg_2SiO_4 is much more closely-packed than Zn_2SiO_4 -II. Both Mg and Si atoms in $I-42d$ -type Mg_2SiO_4 are eight-fold coordinated, while Zn and Si atoms in Zn_2SiO_4 -II are four-fold coordinated (*i.e.* in tetrahedra). The crystal structures of $I-42d$ -type Mg_2SiO_4 and $P2_1/c$ -type MgSi_2O_5 together with the corresponding typical local structures are shown in figure 4, and the structural parameters are given in table 4.

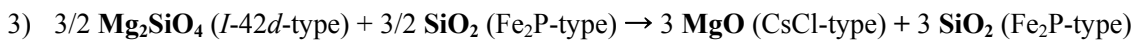
The enlarged *composition space* of possible structures, now reveals a more complex three-step dissociation process: MgSiO_3 PPv first decomposes into two phases at 0.77 TPa, one rich (poor) and one poor (rich) in SiO_2 (MgO):



MgSi_2O_5 then breaks down into Mg_2SiO_4 and SiO_2 at 1.25 TPa:



The complete dissociation into oxides then takes place at 3.09 TPa:



This sequence of transitions is shown in figure 4(c). The dissociation starts at 0.77 TPa and is completed at ~ 3 TPa. This pressure range is expected to change somewhat at high temperatures though. This prediction contrasts with the direct dissociate previously predicted at 1.21 TPa [33] and the two-step ex-solution of MgO predicted between 0.90 and 2.1 TPa [34]. In overall, these results suggest that more

complex sequences of phase transitions could be found by considering intermediate phases with different compositions. The large ionic (LDA) gaps of at least 5 eV found in all phases suggest that phases with different molar fractions of MgO and SiO₂ with even more complex structures are the most natural candidates for future investigations.

In summary, we showed that the adaptive-GA is an efficient scheme for complex crystal structure prediction. The use of adjustable classical potentials in the internal loop of the adaptive-GA improves the speed and efficiency of the search by several orders of magnitude without compromising the DFT accuracy of the final result. Its performance was demonstrated in studies of complex binary and ternary intermetallic alloys. The pressure induced dissociation of MgSiO₃, the major end-member phase of the Earth mantle, into elementary oxides at TPa pressures was also investigated. A three-step dissociation process happening between 0.44 and 3.09 TPa involving complex crystal structures and compositions was identified. Structure prediction in the Mg-Si-O systems is an outstanding example of materials discovery at extreme conditions of planetary interiors where a wealth of novel phases with exotic properties [33] is expected to exist. The adaptive-GA combined with peta-scale computing power is an invaluable method to search for these phases.

Work at Ames Laboratory was supported by the US Department of Energy, Basic Energy Sciences, Division of Materials Science and Engineering, under Contract No. DE-AC02-07CH11358, including a grant of computer time at the National Energy Research Supercomputing Centre (NERSC) in Berkeley, CA. Work at University of Minnesota was supported by NSF/EAR 1047629. Computations were performed at the Minnesota Supercomputing Institute and at the Laboratory for Scientific Computing and Engineering. SQW also acknowledges financial support from the National Natural Science Foundation of China (No. 11004165).

References

- [1] Maddox J 1988 Crystals from First Principles *Nature* **335** 201
- [2] Eberhart M E and Clougherty D P 2004 Looking for Design in Materials Design *Nature Mater.* **3** 659-661

- [3] Kirkpatrick S, Gelatt Jr C D and Vecchi M P 1983 Optimization by Simulated Annealing *Science* **220** 671-680
- [4] Wille L T 1986 Searching Potential Energy Surfaces by Simulated Annealing *Nature* **324** 46-48
- [5] Doll K, Schön J C and Jansen M 2007 Global Exploration of the Energy Landscape of Solids on the Ab Initio Level *Phys. Chem. Chem. Phys.* **9** 6128-6133
- [6] Deaven D M and Ho K M 1995 Molecular Geometry Optimization with a Genetic Algorithm *Phys. Rev. Lett.* **75** 288-291
- [7] Woodley S M, Battle P D, Gale J D and Catlow C R A 1999 The Prediction of Inorganic Crystal Structures Using a Genetic Algorithm and Energy Minimisation *Phys. Chem. Chem. Phys.* **1** 2535-2542
- [8] Harris K D M, Johnston R L and Kariuki B M 1998 The Genetic Algorithm: Foundations and Applications in Structure Solution from Powder Diffraction Data *Acta Crystallogr.* **A54** 632-645
- [9] Woodley S M 2004 Prediction of Crystal Structures Using Evolutionary Algorithms and Related Techniques *Struct. Bonding* **110** 95-132
- [10] Oganov A R and Glass C W 2008 Evolutionary Crystal Structure Prediction as a Tool in Materials Design *J. Phys.: Condens. Matter* **20** 064210
- [11] Lyakhov A O, Oganov A R, Stokes H. and Zhu Q 2013 New Developments in Evolutionary Structure Prediction Algorithm USPEX *Comp. Phys. Comm.* **184** 1172-1182
- [12] Ji M, Umemoto K, Wang C Z, Ho K M and Wentzcovitch R M 2011 Ultrahigh-Pressure Phases of H₂O Ice Predicted Using an Adaptive Genetic Algorithm *Phys. Rev. B* **84** 220105(R)
- [13] Wu S Q, Umemoto K, Ji M, Wang C Z, Ho K M and Wentzcovitch R M 2011 Identification of Post-Pyrite Phase Transitions in SiO₂ by a Genetic Algorithm *Phys. Rev. B* **83** 184102
- [14] Wales D and Doye J 1997 Global Optimization by Basin-Hopping and the Lowest Energy Structures of Lennard-Jones Clusters Containing up to 110 Atoms *J. Phys. Chem. A* **101** 5111-5116
- [15] Goedecker S 2004 Minima Hopping: An Efficient Search Method for the Global Minimum of the Potential Energy Surface of Complex Molecular Systems *J. Chem. Phys.* **120** 9911-9917
- [16] Wang Y, Lv J, Zhu L and Ma Y 2010 Crystal Structure Prediction via Particle-Swarm Optimization *Phys. Rev. B* **82** 094116
- [17] Wang Y, Lv J, Zhu L and Ma Y 2012 CALYPSO: A Method for Crystal Structure Prediction *Comp. Phys. Commun.* **183** 2063-2070
- [18] Pickard C J and Needs R J 2011 Ab Initio Random Structure Searching *J. Phys. Condens. Matter* **23** 053201
- [19] Brommer P and Gahler F 2007 Potfit: Effective Potentials from Ab-Initio Data *Modelling Simul. Mater. Sci. Eng.* **15** 295-304

- [20] Brommer P and Gahler F 2006 Effective Potentials for Quasicrystals from Ab-Initio Data *Phil. Mag.* **86** 753-758
- [21] Giannozzi P *et al.* 2009 QUANTUM ESPRESSO: a Modular and Open-Source Software Project for Quantum Simulations of Materials *J. Phys.: Condens. Matter* **21** 395502
- [22] Kresse G and Furthmuller J 1996 Efficient Iterative Schemes for Ab Initio Total-Energy Calculations Using a Plane-Wave Basis Set *Phys. Rev. B* **54** 11169-11186
- [23] Kresse G and Furthmuller J 1996 Efficiency of Ab-Initio Total Energy Calculations for Metals and Semiconductors Using a Plane-Wave Basis Set *Comput. Mater. Sci.* **6** 15-50
- [24] Cromer D T and Herrington K 1955 The Structures of Anatase and Rutile *J. Am. Chem. Soc.* **77** 4708-4709
- [25] Vegard L 1916 Results of Crystal Analysis *Philos. Mag.* **32** 505-518
- [26] Buschow K H J, Wernick J H and Chin G Y 1978 Note on the Hf-Co Phase Diagram *J. Less-Common Met.* **59** 61-67
- [27] Voroshilov Y V, Krypyakevych P I and Kuz'ma Y B 1971 Crystal structures of $ZrCo_3B_2$ and $HfCo_3B_2$ *Sov. Phys. Crystallogr.* **15** 813-816
- [28] <http://kepler.nasa.gov/>
- [29] http://www.esa.int/Our_Activities/Space_Science/COROT
- [30] Murakami M, Hirose K, Kawamura K, Sata N and Ohishi Y 2004 Post-Perovskite Phase Transition in $MgSiO_3$ *Science* **304** 855-858
- [31] Oganov A R and Ono S 2004 Theoretical and Experimental Evidence for a Post-Perovskite Phase of $MgSiO_3$ in Earth's D" Layer *Nature* **430** 445-448
- [32] Tsuchiya T, Tsuchiya J, Umemoto K and Wentzcovitch R M 2004 Phase Transition in $MgSiO_3$ Perovskite in the Earth's Lower Mantle *Earth Planet. Sci. Lett.* **224** 241-248
- [33] Umemoto K, Wentzcovitch R M and Allen P B 2006 Dissociation of $MgSiO_3$ in the Cores of Gas Giants and Terrestrial Exoplanets *Science* **311** 983-986
- [34] Umemoto K and Wentzcovitch R M 2011 Two-Stage Dissociation in $MgSiO_3$ Post-Perovskite *Earth Planet. Sci. Lett.* **311** 225-229
- [35] Mehl M J, Cohen R E and Krakauer H 1988 Linearized Augmented Plane Wave Electronic Structure Calculations for MgO and CaO *J. Geophys. Res.* **93** 8009
- [36] Karki B B, Stixrude L, Clark S J, Warren M C, Ackland G J and Crain J 1997 Structure and Elasticity of MgO at High Pressure *Am. Mineral.* **82** 51-60
- [37] Oganov A R, Gillan M J and Price G D 2003 Ab Initio Lattice Dynamics and Structural Stability of MgO *J. Chem. Phys.* **118** 10174-10182

- [38] Wu Z, Wentzcovitch R M, Umemoto K, Li B, Hirose K and Zheng J C 2008 Pressure-Volume-Temperature Relations in MgO: An Ultrahigh Pressure-Temperature Scale for Planetary Sciences Applications *J. Geophys. Res.* **113** B06204
- [39] Tsuchiya T and Tsuchiya J 2011 Prediction of a Hexagonal SiO₂ Phase Affecting Stabilities of MgSiO₃ and CaSiO₃ at Multimegabar Pressures *Proc. Nat. Acad. Sci.* **108** 1252-1255
- [40] Marumo F and Syono Y 1971 The Crystal Structure of Zn₂SiO₄-II, a High-Pressure Phase of Willemite *Acta Cryst.* **B27** 1868-1870